

## Route-planning in output-material-flow operations using side-headlands

Santiago Focke Martinez<sup>1</sup> and Joachim Hertzberg<sup>1,2</sup>

**Abstract:** This paper presents an extension to a previously presented planning tool which was developed to generate routes for the machines participating in output-material-flow operations. The extension refers to the support of a headland region consisting of a set of partial side-headlands, comprised by main headlands, located in the sides of the field where inner-field tracks end; and connecting headlands, which border the field boundary and connect the main headlands. Eleven fields were used to test the corresponding tool updates in the planning process, including the geometric representation of the field with the new headland type, and the route planning for a harvesting test-scenario with one non-capacitated harvester and two transport vehicles.

**Keywords:** route planning, Precision Farming, Smart Farming

### 1 Introduction

In-field route planning for arable farming operations has been a focus of research in recent years aiming to improve the efficiency of the process in terms of operational costs, energy consumption, in-field transit, and soil compaction, among others [Nø22; Mo20; NZ20]. Current research deals with input-, output-, and neutral-flow operations, where both capacitated and non-capacitated machines are involved. A planning tool was previously presented [Fo21; FH22], which was developed to generate routes for the machines participating in output-material-flow operations (e.g., harvesting) following different optimization criteria. However, the tool was limited to the generation and usage of a headland that surrounds the main field region (referred here as inner-field) with a set of closed surrounding headland tracks (passes) determined by the desired headland width and the working-width of the machine working the field. This tool was further developed to generate and use a new type of headland region, which comprises a set of main headlands that are located at ends of the inner-field tracks, and a set of single-track-headlands bordering the field boundary connecting the main headlands. Thanks to the latter headlands, it is possible to cover the headland region continuously without leaving the field. Compared to the complete surrounding headland, using the presented headland type will result in a lower overall headland area, and consequently, a higher inner-field area.

This paper presents a brief overview of the route planning tool focusing on the updates to adopt the new headland type in the planning process. The updates were tested by planning

---

<sup>1</sup> German Research Centre for Artificial Intelligence (DFKI), PBR, Berghoffstraße 11, 49090 Osnabrück, santiago.focke@dfki.de

<sup>2</sup> University of Osnabrück, Berghoffstraße 11, 49090 Osnabrück, joachim.hertzberg@uos.de

the routes of an output-material-flow case scenario on 11 real field geometries with different shapes and sizes, involving one non-capacitated primary machine (*PM*) performing the work in the field and two service units (*SU*) for the overload of material from the *PM* and its transportation to an unloading location. Exemplary results of the planning process are presented, followed by limitations, discussion, and future work.

## 2 Methods

The overall route planning process of the presented tool is divided into three main steps: 1) the generation of the field geometries, including the headland and inner-field boundaries and tracks; 2) the generation of the so-called ‘base’ route of the primary machine (*PM*) working in the field; and 3) the final planning of the routes for all machines participating in the operation, including extraction of material, overloading, and transit to and from the unloading locations. This section is focused on the updates developed to adopt the new headland type; further details on the planning process can be found in [Fo21; FH22].

To generate the field geometric representation in step 1), a reference line for the inner-field (*IF*) tracks is given as an input. The *IF* tracks are generated by extending said reference line and recursively translating it into a distance equal to the working width of the primary machine (*PM<sub>ww</sub>*) until the *IF* region is completely covered. An initial set of *IF* tracks is generated to determine the sides of the field where the main headlands (*MHLs*) will be located. Next, the boundaries of the main headlands are generated based on the desired headland width, followed by the generation of the corresponding tracks with a track width equal to the *PM<sub>ww</sub>* (the resulting headland width will be a multiple of *PM<sub>ww</sub>*). These tracks are generated so that the distance between the track-ends and the headland boundary is equal to *PM<sub>ww</sub>*. Next, the connecting headlands (*CHLs*) are generated, which are located in the remaining sides of field boundary and comprise only one track. The *CHL* tracks also have a width equal to the *PM<sub>ww</sub>*, but the track-ends intersect the corresponding headland boundary. Finally, the boundary of the *IF* region is obtained by subtracting the headland areas from the field boundary, and the *IF* tracks are regenerated to cover this new boundary. Depending on the shape and area of the field boundary and desired headland width, three cases of geometric representation result from step 1). If the boundaries of the two *MHLs* do not intersect, the set of headlands will comprise two *MHLs* connected by two *CHLs* (type M2C2). If the boundaries of the two initially generated *MHLs* intersect in one side, these headlands will be merged into a single *MHL*, and one *CHL* will connect both sides of the *MHL* (type M1C1). A third case arises when both sides of the initially generated *MHLs* intersect; in this case, a complete surrounding headland is generated, and the planning processes presented in [Fo21] will be followed.

In step 2), the base route of the *PM* is generated, which represents the route that the *PM* will follow to cover the field area without considering the capacity constraints or unloading activities. As on [Fo21], the base route will cover the headland region first, followed by the *IF* region. The *PM* will start from one of the two ends of the outermost track of the first headland to be worked. The first headland will be automatically selected

based on the locations of the PM and the field access points, and can be either a MHL or a CHL. At least one access point must be located near an outer-most headland track-end. The PM will work the headland from the outermost track to the innermost track and then continue with the non-worked adjacent headland which is closest to the last worked track point. This process will be repeated until all headlands are covered. Thanks to the CHLs, it is possible to work all headlands continuously; however, if a MHL is neither the first nor the last headland to be worked, and its number of tracks is even, the PM will have to transit over one already-worked track to reach the next CHL, which should be avoided not to introduce undesired non-working transit. In the connections from a CHL to an MHL, the PM will work a segment of the MHL before starting to work on the MHL outermost track. This segment is built by connecting the track-ends of the MHL that are closest to the CHL end point, from the innermost- to the outermost- track. Once all headlands are worked, the PM will cover the IF following the IF tracks from one side of the field to the other, starting with the track closest to the last worked headland point (as done in [Fo21]). The transit between IF tracks is done over the headland region either by direct connections using Dubins paths or via connected headland tracks.

Step 3) follows the same procedure as presented in [Fo21; FH22] for the two supported case scenarios, namely a) one capacitated PM that works the field and transports the material; and b) one non-capacitated PM that works the field in coordination with one or more capacitated service units (SU). First, the search graph that is used for in-field path planning is built based on the generated geometries and the base route. Next the working windows for each capacitated machine are computed based on the container capacity and the amount of material in the field. The working windows divide the process into a set of sub-processes (tours), each of them involving transit to the field, working of the field and overloading of material (if applicable), and transit to an unloading location (e.g., a clamp next to the field or a silo). The routes generated in each tour are finally combined to obtain the machine routes, which are smoothed based on the corresponding turning radii.

### 3 Results

The new updates were tested by planning a harvesting operation on 11 fields with varying shapes, belonging to cases M2C2 and M1C1. The operation consisted of one non-capacitated harvester (PM) with a working width of 6m, and two transport vehicles (SU) with a container capacity of 10t. A headland width of 24m was selected, resulting in five tracks per MHL. Tab. 1 contains the geometric properties of the test fields, including the total field areas, the areas of the resulting MHL-, CHL-, and IF- regions, and the number of generated side-headlands. Fig. 1 shows the resulting geometries for six of the test fields.

For the route planning, an average yield mass of 50t/ha was selected. The routes were planned aiming to optimize the overall duration of the harvesting operation [FH22], and the switch between overloading windows from one SU to the other was not restricted to the IF track-ends. Results for the planning process in field F9 are presented next. Fig. 2

shows the resulting geometric representation and the generated graph for this field. The harvester route and the route of one of the transport vehicles are depicted in Fig. 3.

Id	FA[m <sup>2</sup> ]	P/A [m <sup>-1</sup> ]	IFA[m <sup>2</sup> ] (% FA)	MHLA[m <sup>2</sup> ] (% FA)	CHLA[m <sup>2</sup> ] (% FA)	HL type
F1	117120	0.013	97342 (83.1%)	14402 (12.3%)	5376 (4.6%)	M2C2
F2	14688	0.038	4914 (33.5%)	8958 (61.0%)	816 (5.6%)	M1C1
F3	27630	0.028	13600 (49.2%)	12704 (46.0%)	1326 (4.8%)	M1C1
F4	108840	0.014	85894 (78.9%)	18566 (17.1%)	4380 (4.0%)	M2C2
F5	23117	0.031	9549 (41.3%)	12768 (55.2%)	800 (3.5%)	M1C1
F6	32072	0.035	21279 (66.3%)	6097 (19.0%)	4696 (14.6%)	M2C2
F7	9061	0.047	4172 (46.0%)	3858 (42.6%)	1032 (11.4%)	M2C2
F8	146962	0.011	118801 (80.8%)	23974 (16.3%)	4186 (2.8%)	M2C2
F9	15609	0.033	7908 (50.7%)	6661 (42.7%)	1041 (6.7%)	M2C2
F10	55231	0.018	38547 (69.8%)	14716 (26.6%)	1968 (3.6%)	M2C2
F11	49633	0.021	37815 (76.2%)	8015 (16.1%)	3803 (7.7%)	M2C2

Tab. 1: Test fields. FA: Field Area; P/A: Perimeter/Area; IFA: *IF* Area, MHLA: Area of *MHLs*; CHLA: Area of *CHLs*; %FA: % of field area; HL type: headland type

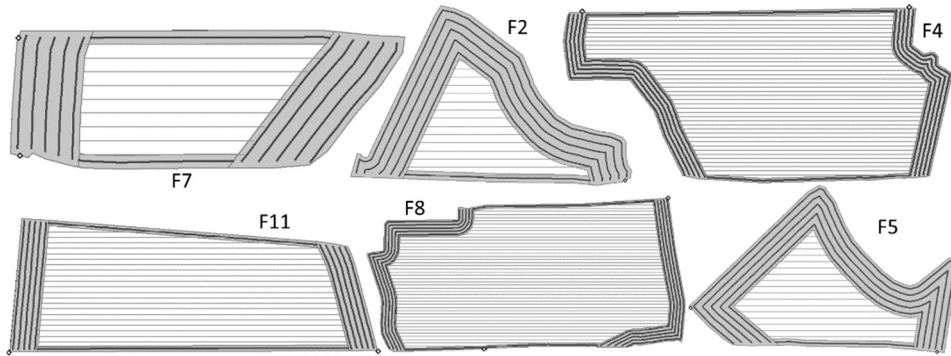


Fig. 1: Field geometries: Headlands (grey background) and Inner-field (white background) with corresponding tracks. Note: the field images are not in the same scale (see Tab. 1)

Because the planner does not support complex manoeuvres involving reverse driving, some limitations arise during the base-route planning. As can be seen in Fig. 3 (left), the connection between headland tracks is done by a simple connecting path between track-ends (with reduced speed). In practice, however, it is expected that the driver needs to perform more complex manoeuvres to harvest these small segments whilst remaining inside the field boundary. This also applies for other headland track segments with steep turns. Another current limitation arises when the field boundary segments adjacent to the *CHLs* are not fairly parallel to the reference line, causing some *IF* tracks-ends to be

adjacent to a CHL and not to an MHL. Such case can be seen, for instance, in field F11. Depending on the geometries of the adjacent CHL and the working direction of the IF track, complex manoeuvres and/or longer transit segments over the headland tracks might be needed to connect to the IF track. As a result, the planned connection paths might significantly differ to the paths driven in practice. This drawback can be resolved by removing the conflicting CHL and combining the two MHLs to ensure that all IF track-ends are adjacent to an MHL.

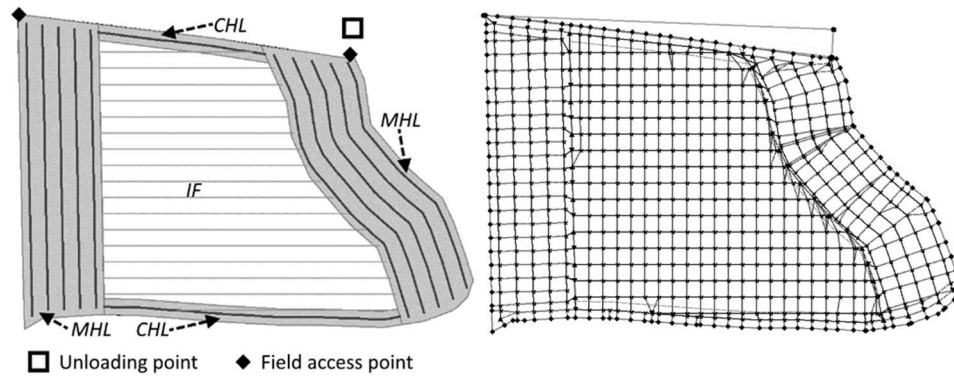


Fig. 2: Field F9 geometries (left) and graph (right)

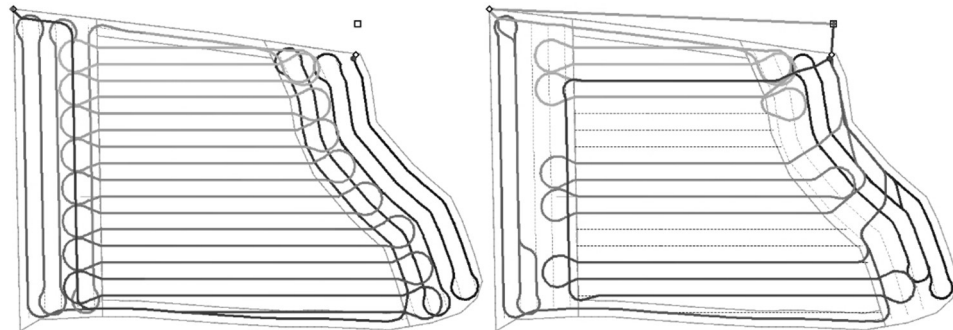


Fig. 3: Harvester route (left); transport vehicle route (right)

## 4 Conclusions

This paper presented an extension to the planning tool from [Fo21; FH22] to support in-field route planning with a new type of headland region. This region consists of a set of partial headlands, comprised by main headlands (located at the inner-field track-ends) and connecting headlands (bordering the field boundary and connecting the main headlands). This headland type results in a reduced overall headland region focused on the areas where the primary machine performs the turns to transit between IF tracks.

The tool updates were tested by planning a harvesting campaign in 11 test fields with one non-capacitated harvester and two transport vehicles. The results show that the generated field geometric representation is highly dependent on the headland width and the field shape and size. The limitations of the planning component related to complex manoeuvres involving reverse driving translated into the generation of route segments that are expected to differ from real driving on the field. However, the tool is currently meant to be used as a reference global planner, hence it is expected that the driver will perform the appropriate manoeuvres to satisfy the field and operation constraints. Aside from the presented limitations, the tool satisfyingly planned the routes for all participating machines in all test fields. The preliminary results suggest that the usage of the presented headland type should depend on the field base geometries (shape, access points, etc.) to avoid the introduction of complex manoeuvring for the drivers and long non-working travel distances. Future work includes improvements on the headlands generation to ensure that all IF track-ends are adjacent to an MHL, as well as the further testing of the planning tool in different output-material-flow operations and traffic analysis comparing the two supported headland types.

**Acknowledgements:** The SOILAssist project is funded by the Federal Ministry of Education and Research (BMBF) within the framework of the BonaRes-initiative (grant no. 031B1065B). The DFKI Niedersachsen (DFKI NI) is sponsored by the Ministry of Science and Culture of Lower Saxony and the VolkswagenStiftung.

## Bibliography

- [FH22] Focke Martinez, S.; Hertzberg, J.: Route-planning in output-material-flow arable farming operations aiming for soil protection, in 42. GIL-Jahrestagung, Künstliche Intelligenz in der Agrar- und Ernährungswirtschaft, Bonn, 2022.
- [Fo21] Focke Martinez, S. et.al: Overview of a route-planning tool for capacitated field processes in arable farming, in 41. GIL-Jahrestagung, Informations- und Kommunikationstechnologie in kritischen Zeiten, Bonn, 2021.
- [Mo20] Moysiadis, V. et.al: Mobile Robotics in Agricultural Operations: A Narrative Review on Planning Aspects. *Applied Sciences* 10/10, p. 3453, 2020.
- [Nø22] Nørremark, M. et.al: In-Field Route Planning Optimisation and Performance Indicators of Grain Harvest Operations. *Agronomy* 12/5, p. 1151, 2022.
- [NZ20] Nilsson, R.S.; Zhou, K. Decision Support Tool for Operational Planning of Field Operations. *Agronomy* 10/2, p. 229, 2020.